Sensor Modeling for Aerial Triangulation with Three-Line-Scanner (TLS) Imagery

Armin Gruen & Zhang Li, Zürich

Summary: This article describes the sensor modeling and the photogrammetric triangulation procedure for the TLS (Three-Line-Scanner) system. This system is a new airborne digital sensor, developed by STARLABO Corporation, Tokyo jointly with the Institute of Industrial Science, University of Tokyo. It utilizes the Three-Line-Scanner principle to capture digital image triplets in along-strip mode. The imaging system contains three times three (RGB) one-dimensional CCD arrays, with 10 200 pixels of 7 μm each, mounted parallel to each other in the focal plane. They produce seamless high-resolution images (5–10 cm footprint on the ground) with three viewing directions (forward, nadir and backward). In order to get precise attitude data and high quality image data from an aerial platform, a high quality stabilizer stabilizes the camera and outputs attitude data at 500 Hz. A Trimble MS750 serves as Rover GPS and collects L1/L2 kinematic data at 5 Hz and another Trimble MS750 serves as Base GPS on the ground.

The position and attitude elements measured by the on-board GPS/INS do not refer to the perspective center of the imaging camera. Additionally, there is a boresight misalignment between the axes of the INS and the camera. These translational and rotational offsets have been taken into account in our sensor model and triangulation procedures. In our experiments, the following 3 trajectory models are evaluated: (a) Direct georeferencing with stochastic exterior orientations (DGR), (b) Piecewise Polynomials with kinematic model up to second order and stochastic zero and first order continuity constraints (PPM) and (c) Lagrange Polynomials with variable orientation fixes (LIM).

With different numbers and distributions of control points and tie points, 4.9–6.3 cm and 8.6–9.4 cm absolute accuracy in planimetry and height is achieved using the DGR model under

Zusammenfassung: *Sensormodellierung für die Aerotriangulation mit Bildern von Dreizeilenkammern (TLS).* Dieser Beitrag beschreibt die Modellierung des TLS (Three-Line-Scanner)- Systems und die dafür entwickelten Verfahren zur photogrammetrischen Triangulation. Dieses System, dessen Kernstück eine neue digitale Luftbildkamera darstellt, wurde von der Firma STARLABO Corporation, Tokyo in Zusammenarbeit mit dem Institut of Industrial Science, University of Tokyo entwickelt. Es arbeitet mit dem Drei-Zeilen-Prinzip, um digitale Mehrfachbildstreifen im simultanen Streifenverfahren zu generieren. Das Abbildungssystem besteht aus drei Paketen von je drei (RGB) eindimensionalen Linear Array CCD-Sensorelementen, mit 10 200 Pixel pro Linie und einer Pixelgröße von 7 μm, welche parallel zueinander in der Bildebene angeordnet sind. Diese produzieren eine simultane Dreifachabdeckung des Bodens (Vorwärts, Nadir, Rückwärts) mit hochauflösenden Bildern von 5 bis 10 cm Bodenpixelgröße. Das System wird standardmäßig auf einem Helikopter montiert, aber auch die Integration auf einer Flugzeugplattform ist möglich. Um genaue Winkelwerte für die äußere Orientierung und eine sehr gute Bildqualität bereits bei den Rohbildern zu bekommen, wird ein hochqualitativer Stabilisator mit einer Outputrate von 500 Hz eingesetzt. Ein Trimble MS750 dient als Rover GPS und sammelt L1/L2 kinematische Daten mit 5 Hz im differentiellen Modus.

Da die Daten der äußeren Orientierung sich nicht auf das Projektionszentrum der Kamera beziehen, müssen entsprechende Korrekturen in Kalibrierungs-, Georeferenzierungs- und Triangulationsverfahren eingebaut werden. Für diese Aufgaben haben wir insgesamt drei Trajektorienmodelle entworfen, implementiert und untersucht:
a) Direkte Georeferenzierung mit stochastischer äußerer Orientierung (DGR),
b) Stückweise Polynome, aufbauend auf einem

the condition that the GPS/camera displacement corrections have been applied. Moreover, with different numbers of spline sections or orientation fixes, 2.6–6.0 cm and 4.9–11.7 cm absolute accuracy in planimetry and height is attained using the PPM and LIM models. These results show that a ground point determination of 0.5–1.2 pixel accuracy in planimetry and 0.7–2.1 pixel accuracy in height has been achieved. The orientation parameter determination using the DGR model has the advantage of stability and needs less control points, but the obtained accuracy is better with the PPM and LIM models. This however is penalized by the need to have more well-distributed control and tie points.

kinematischen Modell zweiter Ordnung und stochastische Stetigkeitsbedingungen nullter und erster Ordnung (PPM), und
(c) Lagrange Polynome mit Orientierungsabschnitten variabler Länge (LIM).

Diese Trajektorienmodelle wurden als drei verschiedene Triangulationsverfahren realisiert und empirisch, das heißt mit Testfelddaten, untersucht. Unter Benutzung einer unterschiedlichen Anzahl und Verteilung von Passpunkten und Verknüpfungspunkten wurden mit der DGR-Methode Lagegenauigkeiten von 4.9–6.3 cm und Höhengenauigkeiten von 8.6–9.4 cm erreicht, unter der Voraussetzung, dass die GPS/Kamera Offsetkorrekturen a priori angebracht wurden. Mit den PPM- und LIM-Methoden, unter Benutzung einer unterschiedlichen Anzahl von Splinesektionen und variablen Längen von Orientierungsabschnitten, wurden Lagegenauigkeiten von 2.6–6.0 cm und Höhengenauigkeiten von 4.9–11.7 cm erreicht. Diese Ergebnisse zeigen, dass Bodenpunktgenauigkeiten von 0.5–1.2 Pixel in der Lage und 0.7–2.1 Pixel in der Höhe durchaus realistisch sind.

Dabei hat die DGR-Methode den Vorteil der generellen Einfachheit und Stabilität und benötigt die geringste Anzahl Passpunkte. Die beiden anderen Methoden dagegen haben ein höheres Genauigkeitspotenzial, aber ihr Einsatz erfordert eine ausgefeilte interne Qualitätskontrolle.

1   Introduction

During the last decade, in photogrammetry and remote sensing high spatial resolution digital sensors are being developed to collect panchromatic and multispectral imagery. Currently, most of these digital sensors are based on the Three-Line-Scanner principle. The use of three or more linear arrays in pushbroom mode is due to at least three good reasons: (a) matrix CCD array imaging systems with a comparable size are still not available, (b) the line sensors allow for a more flexible camera design and, (c) this new imaging mode allows for new and more powerful algorithmic approaches in data processing. Cameras based on linear CCD sensors like the Wide Angle Airborne Camera WAAC (Boerner et al. 1997), the High Resolution Stereo Camera HRSC (Wewel et al. 1999), the Digital Photogrammetric

Assembly DPA (Haala et al. 1998) were the first digital systems being used for airborne applications. The first commercial line scanner Airborne Digital Sensor ADS40 was developed by LH Systems jointly with DLR and was introduced at the XIXth ISPRS Congress in Amsterdam (Reulke et al. 2000, Sandau et al. 2000). In the year 2000, STARLABO Corporation, Tokyo designed a new airborne digital imaging system, the Three-Line-Scanner (TLS) system, jointly with the Institute of Industrial Science, University of Tokyo and completed in the meantime several test flights. The TLS system was originally designed to record line features (roads, rivers, railways, power-lines, etc) only, but later tests also revealed the suitability for general mapping and GIS-related applications. However, this was already conceived by Murai & Matsumoto 2000 and Murai 2001.

Georeferencing the image data of linear scanner systems is more complex compared to standard aerial triangulation. In traditional photogrammetric triangulation, the georeferencing problem is solved indirectly using some well-distributed control points and applying geometric constraints such as collinearity equations between the image points and object points. In principle, this approach can be transfered directly to line scanner imagery, but due to the instability of the platform during the scanning process the geometry of this imagery is much weaker compared to the traditional frame sensor imagery. Basically, the orientation parameters for all the image lines need to be recovered. In satellite platform applications this problem can partly be solved by modeling the trajectory by piecewise polynomial models, due to the fact that there is a high correlation between the orientation parameters of each scan line. In these models, only the polynomial parameters have to be recovered by using the control and tie points. Because of the high dynamics of the airborne environment and platform, the airborne digital sensors have to be integrated with high accuracy INS and GPS systems. This additional information allows for reducing the number of control points and enables even direct georeferencing of the linear array imagery. Nowadays, the integration of INS/GPS using the Kalman filter approach can reach a high absolute accuracy. For GPS, using the differential phase observations with rover-master receiver separation below 30 km, better than 10 cm absolute positional accuracy in airborne kinematic environments can be achieved (CANNON 1994, CRAMER 2000). Using a GPS-updated, high to medium accuracy inertial system for attitude determination, accuracies in the range of 10–30 arc sec can be obtained (SCHWARZ & WEI 1994, SKALOUD 1999, CRAMER 2000). In a combined aerial triangulation approach, these parameters from the integrated INS/GPS system are used as additional weighted observations.

This article deals with the sensor modeling and the high precision georeferencing of the TLS imagery, collected with the Three-Line-Scanner System developed by STARLABO Corporation, Tokyo. The next section describes briefly the TLS system. Then we report about the sensor model. Following that three different trajectory models and the corresponding combined triangulation approaches are introduced. In the final part the experimental results and conclusions will be provided.

2   The TLS System

The TLS (Three-Line-Scanner) system is a new airborne digital sensor, developed by STARLABO Corporation, Tokyo (MURAI & MATSUMOTO 2000, MURAI 2001, CHEN et al. 2001). It utilizes the Three-Line-Scanner principle to capture digital image triplets in along-strip mode. The imaging system contains three times three parallel one-dimensional CCD focal plane arrays, with 10 200 pixels of 7 µm each (Fig. 1). The TLS system produces seamless high-resolution images (5–10 cm footprint on the ground) with three viewing directions (forward, nadir and backward). There are two configurations for image acquisition. The first configuration ensures the stereo imaging capability, in which the three CCD arrays working in the green channels are read out with stereo angles of about 21 degrees.

The second configuration uses the RGB CCD arrays in nadir direction to deliver color imagery. In order to get precise attitude data and good quality raw image data from an aerial platform, a high quality stabilizer is used for the camera and outputs attitude data at 500 Hz. A Trimble MS750 serves as Rover GPS and collects L1/L2 kinematic data at 5 Hz and another Trimble MS750 serves as Base GPS on the ground. For the TLS sensor and imaging parameters see Tab. 1.

The TLS imaging system does not use the highest quality gyro system to achieve highly precise attitude data over long flight lines. Instead, a combination of a high local accuracy INS with the high global accuracy GPS is exploited. The rover GPS is installed on the top of the aircraft the INS and the TLS camera are firmly attached together.
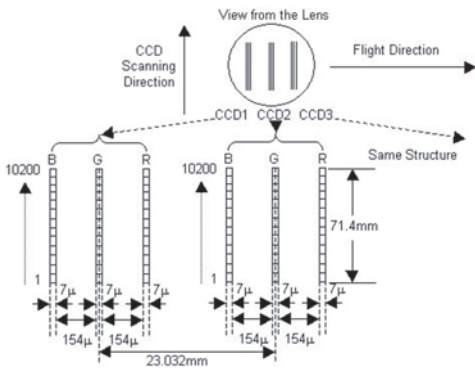
Fig. 1: TLS CCD sensor configuration.

Fig. 2: System configuration of the TLS system.

Tab. 1: TLS sensor and imaging parameters.

focal length	60.0 mm
number of pixels per array	10200
pixel size	7 µm
number of CCD focal plane arrays	3
stereo view angle	21/42° *
Field of view	61.5°
instantaneous field of view	0.0065°
scan line frequency	500 HZ

* forward-nadir/forward-backward stereo view angle

Fig. 2 shows the configuration of the TLS components. After the collection of the GPS/INS raw data, the kinematic position and attitude data are calculated, but without use of a Kalman filter approach or anything equivalent. This results in large drift values for the INS observations, which currently have to be recovered, together with possible other systematic errors, by triangulation.

Unlike with frame-based photography, the three-line geometry is characterized by a nearly parallel projection in the flight direction and perspective projection perpendicular to that. Our sensor model for the TLS images is based on modified collinearity equations and uses different forms of trajectory models. These models are used for the improvement of the measured exterior orientation parameters for each scan line of TLS images by a modified photogrammetric bundle adjustment procedure, called TLS-LAB.

3   Sensor Modeling

Each scan line of the TLS image is collected in a pushbroom fashion at a different instant of time. Therefore, there is in principle a different set of values for the six exterior orientation parameters for each scan line. A good mathematical sensor model is needed to improve the time-dependent orientation elements of the TLS trajectory by photogrammetric triangulation.

At any given instant of time we can imagine the TLS CCD sensors to be positioned perpendicular to its flight trajectory at the instantaneous perspective center (Fig. 3). At
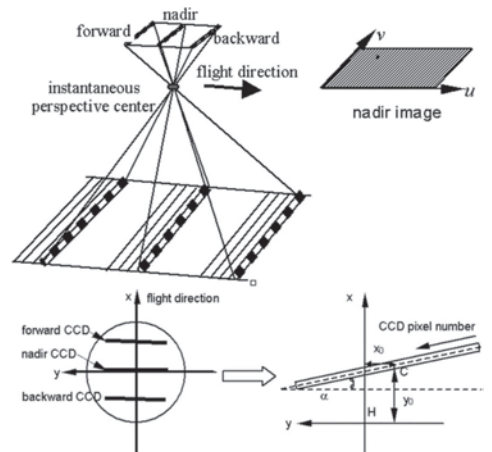

Fig. 3: TLS CCD sensor coordinate system definition and interior orientation parameters.
C: Center point of CCD linear array
H: Principal point
α: Inclination of CCD array to y-axis

this instant of time three lines of 10 200 pixels each are acquired. With the movement of the aircraft three TLS image strips are constructed. In the TLS imagery the pixel coordinates of one certain point are given by its digital image column v and the scan line number u. We define the image coordinate system (x, y) as having its origin in the principle point of the focal plane and its x-axis perpendicular to the nadir CCD line. It is obvious that the image coordinates (x, y) of an image point are only related to the pixel coordinate v and the interior orientation parameters. After the interior orientation parameters and the lens distortion of the TLS camera have been estimated in the laboratory by a collimator device, the image coordinates (x, y) of a point can be computed by the following equations with respect to its pixel coordinate v (including a correction for radial distortion Δr):

$$\begin{cases} x' = x_0 + (v - Midv) \times ps \times \sin \alpha \\ y' = y_0 + (v - Midv) \times ps \times \cos \alpha \end{cases}$$

$$\begin{cases} x = x' + \Delta r \times x'/r = I_x(v) \\ y = y' + \Delta r \times y'/r = I_y(v) \end{cases} \quad (1)$$

and
$$\Delta r = a_1 r + a_3 r^3 + a_5 r^5$$
$$r = \sqrt{x'^2 + y'^2}$$

(x_0, y_0) are the image coordinates of the center of the CCD arrays, α is the inclination angle for the forward and backward CCD arrays to the image y axis, a_1, a_3 and a_5 are radial symmetric lens distortion correction coefficients, $Midv$ is the number of the CCD central pixel and ps is the pixel size (Fig. 3).

To relate the image coordinates (x, y) to the object coordinates (X, Y, Z) of a terrain point at any given instant, the following collinearity equations are used:

$$\begin{bmatrix} X \\ Y \\ Z \end{bmatrix} = \begin{bmatrix} X_0 \\ Y_0 \\ Z_0 \end{bmatrix}_N + \lambda R(\omega, \varphi, \kappa)_N \begin{bmatrix} x \\ y \\ -c \end{bmatrix} \quad (2)$$

Here c is the calibrated camera constant; X_0, Y_0, Z_0, ω, φ and κ are the exterior orientation parameters belonging to the Nth scan

cycle. Assuming a constant scanning frequency f_s, the orientations parameters are functions of the pixel coordinate u:

$$u = f_s t \quad (3)$$

These orientation parameters can be measured by the onboard GPS/INS system directly, or estimated by means of a photogrammetric triangulation procedure with some well-distributed control points. The directly measured position and attitude elements (X_{GPS}, Y_{GPS}, Z_{GPS}, ω_{INS}, φ_{INS}, κ_{INS}) from the GPS/INS system do not refer to the perspective center of the imaging camera. The GPS antenna and the center of the INS unit are displaced from the camera, resulting in translational and rotational offsets (Fig. 2). Additionally, there is a boresight misalignment between the axes of the INS and the camera. These translational and rotational displacements should be corrected in order to obtain correct exterior orientation parameters for the instantaneous perspective center:

$$\begin{cases} X_0(t) = X_{GPS}(t) + \Delta X(t) \\ Y_0(t) = Y_{GPS}(t) + \Delta Y(t) \\ Z_0(t) = Z_{GPS}(t) + \Delta Z(t) \end{cases} \quad (4a)$$

$$\begin{cases} \omega(t) = \omega_{INS}(t) + \Delta \omega_{INS} \\ \varphi(t) = \varphi_{INS}(t) + \Delta \varphi_{INS} \\ \kappa(t) = \kappa_{INS}(t) + \Delta \kappa_{INS} \end{cases} \quad (4b)$$

Where (ΔX, ΔY, ΔZ) are translational displacement corrections between the GPS receiver and the TLS camera; ($\Delta \omega_{INS}$, $\Delta \varphi_{INS}$, $\Delta \kappa_{INS}$) are INS errors including the boresight misalignment angles between the axes of the INS and the TLS camera.

The translational displacement vector between the GPS receiver and TLS camera can be determined using conventional terrestrial surveying methods after the installation of the TLS system in the aircraft. In the TLS system, the stabilizer keeps the camera pointing vertically to the ground in order to get high quality raw images, so the achieved attitude data from INS refers to the INS/camera body and not to the aircraft. For correction of this kind of displacement,

the aircraft attitude data should be recorded and used. In case of the TLS system this is done by mounting three GPS antennas on the aircraft, and deriving the attitude values from their coordinate recordings. We can measure the GPS-INS displacement when the system is in its initial status, then use the recorded aircraft attitude data to calculate the instant GPS-INS displacement at the same frequency as the aircraft attitude data. Using the same method, the INS-camera displacement vector can also be obtained. For the total GPS-camera displacement vector we obtain:

$$\begin{bmatrix} \Delta X(t) \\ \Delta Y(t) \\ \Delta Z(t) \end{bmatrix} = R(\Omega(t),\ \Phi(t),\ K(t)) \begin{bmatrix} T_X \\ T_T \\ T_Z \end{bmatrix}_{GPS/INS} + \begin{bmatrix} 0 \\ 0 \\ s \end{bmatrix}_{INS/CAMERA} \quad (5)$$

Where $(T_X, T_Y, T_Z)^T$ is the translational displacement vector between the GPS receiver and the INS; s is the vertical displacement between the INS and TLS camera. Since it is only about 20.3 cm in length its rotation can be neglected. $(\Omega(t), \Phi(t), K(t))$ are the instantaneous attitude values for the aircraft. Due to the low accuracy of the aircraft attitude data (RMS of the directional values is 0.3°), there should be some residual errors left in the position data for the perspective center of the camera. Assuming the maximum component of GPS-INS displacement vector is 2 meters, the error caused by the directional error of the aircraft attitude data could be $1-3$ cm. This fact should be considered in the TLS sensor modeling.

The rotational offsets, i.e. the boresight misalignment between the INS sensor axes and the camera coordinate system cannot be observed via conventional surveying methods. The attitude errors of the INS system mainly consist of the constant offset (ω_0, φ_0, κ_0) due to the incorrect initial alignment and the drift errors (ω_1, φ_1, κ_1). These errors have to be determined or corrected to obtain correct attitude data (ω, φ, κ).

$$\begin{cases} \Delta\omega_{INS} = \omega_0 + \omega_1 t \\ \Delta\varphi_{INS} = \varphi_0 + \varphi_1 t \\ \Delta\kappa_{INS} = \kappa_0 + \kappa_1 t \end{cases} \quad (6)$$

By combining the equations from (1) to (6), the sensor model can be written as:

$$\begin{bmatrix} X \\ Y \\ Z \end{bmatrix} = \begin{bmatrix} X_{GPS}(t) \\ Y_{GPS}(t) \\ Z_{GPS}(t) \end{bmatrix} + R\begin{pmatrix} \Omega(t) \\ \Phi(t) \\ K(t) \end{pmatrix} \begin{bmatrix} T_X \\ T_Y \\ T_Z \end{bmatrix} + \begin{bmatrix} 0 \\ 0 \\ s \end{bmatrix} + $$
$$+ \lambda R \begin{pmatrix} \omega_{INS} + \omega_0 + \omega_1 t \\ \varphi_{INS} + \varphi_0 + \varphi_1 t \\ \kappa_{INS} + \kappa_0 + \kappa_1 t \end{pmatrix} \begin{bmatrix} x \\ y \\ -c \end{bmatrix} \quad (7)$$

$$Where \quad t = \frac{u}{f_s}; \quad \begin{bmatrix} x \\ y \end{bmatrix} = \begin{bmatrix} I_x(v) \\ I_y(v) \end{bmatrix}$$

This expresses the relationship between the pixel coordinates (u, v) and the object coordinates (X, Y, Z).

Equations (7) are the basic equations in the triangulation approach, which are appended by a trajectory model. The strength of the triangulation process with TLS data lies in the fact that at any instant of time there is only one set of orientations of the aircraft, yet there are three lines of data acquired. Measurements can be made in all three images, enabling each tie point to be located in three images and a good degree of redundancy to be achieved.

So far we have experimented with three different types of trajectory models: (a) Direct georeferencing with stochastic exterior orientations (DGR), (b) Piecewise Polynomials with kinematic model up to second order and stochastic zero and first order continuity constraints (PPM) and (c) Lagrange Polynomials with variable orientation fixes (LIM). The detailed formulation of our trajectory models is given in the next section.

4 Trajectory Models

4.1 *Direct Georeferencing Model (DGR)*

Under the condition that the attitude data of the aircraft was recorded successfully, the translational displacement vector can be cal-

culated and corrections can be made for the TLS positional data (equations (4) and (5)). Considering the errors of the aircraft attitude elements and the GPS errors, the positional data for the whole TLS trajectory can be modeled as:

$$
\begin{aligned}
X_0(t) &= X_{GPS}(t) + X_{off} \\
Y_0(t) &= Y_{GPS}(t) + Y_{off} \\
Z_0(t) &= Z_{GPS}(t) + Z_{off}
\end{aligned}
\tag{8}
$$

Where $(X_{off}, Y_{off}, Z_{off})$ are one set of unknown offset parameters to be estimated for the whole strip. Similarly, the INS error terms $(\Delta\omega, \Delta\varphi, \Delta\kappa)$ can be modeled by equations (6) for the whole trajectory.

Combining equations (6) to (8), the following observation equations for the triangulation procedure of TLS imagery can be formed:

$$
\begin{cases}
v_c = Ax_{off} + B_s x_s + B_d x_d + Cx_g - l_c; & P_c \\
v_s = \qquad\qquad x_s \qquad\qquad\qquad - l_s; & P_s \\
v_d = \qquad\qquad\qquad\qquad x_d \qquad - l_d; & P_d \\
v_g \qquad\qquad\qquad\qquad\qquad\quad x_g - l_g; & P_g
\end{cases}
\tag{9}
$$

The first equation of this system is the linearized observation equation of (7) and x_{off} is the unknown positional offset vector; x_s and x_d are the unknown INS shift and drift terms respectively; x_g is the ground coordinates vector; A, B_s, B_d and C are the corresponding design matrices; v, l and P are the respective residual and discrepancy vectors and weight matrices.

This trajectory model allows the determination of 9 systematic error components, which are the remaining errors after the GPS-camera displacement vector and the INS error terms correction. The INS shift and drift terms and the ground coordinates are treated as stochastic variables. The triangulation procedure based on this trajectory model can thus be used for TLS system calibration and direct georeferencing as well.

4.2 *Piecewise Polynomial Model (PPM)*

The piecewise polynomial model has been often used to model the platform trajectory with respect to time (LEE et al. 2000). In a plain polynomial model, the values of the exterior orientation parameters are written as polynomial functions of time. The bundle adjustment solution determines the polynomial coefficients instead of the exterior orientation parameters themselves. Due to the instability of the high-order polynomial models here, the piecewise polynomial model is used, in which the full complex trajectory is divided into sections, with each section having its own set of low-order polynomials. Continuity constraints on the orientation parameters at the section boundaries ensure that the calculated positions and attitudes are continuous across the boundaries.

The piecewise polynomial model is used to model the translational displacement correction terms $(\Delta X, \Delta Y, \Delta Z)$. The model is described as:

$$
\begin{aligned}
\Delta X(t) &= x_0^k + x_l^k t + x_2^k t^2 \\
\Delta Y(t) &= y_0^k + y_l^k t + y_2^k t^2 \\
\Delta Z(t) &= z_0^k + z_l^k t + z_2^k t^2
\end{aligned}
\tag{10}
$$

for $k = 1, 2, \ldots, n_s$
$\quad n_s = $ *number of polynomial segments*

The INS errors are a function of time and most of the time-dependent errors follow a systematic pattern, so the INS error terms $(\Delta\omega, \Delta\varphi, \Delta\kappa)$ are modeled by equations (6) for the whole trajectory.

The total number of unknown parameters in this piecewise polynomial model with n_s segments is $9 \times n_s + 6$, i.e.

$$
x_0^k, y_0^k, z_0^k, x_1^k, y_1^k, z_1^k, x_2^k, y_2^k, z_2^k;
$$
$$
(k = 1, 2, \ldots \ldots, n_s)
$$
and $\quad \omega_0, \varphi_0, \kappa_0, \omega_1, \varphi_1, \kappa_1$

There are two kinds of constraints that are applied to each parameter at the section boundaries. The zero order continuity constraints ensure that the value of the function computed from the polynomial in every two neighboring sections is equal at their boundaries, i.e.

$$
\begin{cases}
x_0^{k-1} + x_1^{k-1}t + x_2^{k-1}t^2 = x_0^k + x_1^k t + x_2^k t^2 \\
y_0^{k-1} + y_1^{k-1}t + y_2^{k-1}t^2 = y_0^k + y_1^k t + y_2^k t^2 \\
z_0^{k-1} + z_1^{k-1}t + z_2^{k-1}t^2 = z_0^k + z_1^k t + z_2^k t^2
\end{cases}
\tag{11}
$$

$$k = 2, 3, \ldots \ldots, n_s$$

The first order continuity constraint requires that the slope, or first order derivative, of the functions in two adjacent sections is forced to have the same value at their boundary, i. e.

$$\begin{cases} x_1^{k-1} + 2x_2^{k-1}t = x_1^k + 2x_2^k t \\ y_1^{k-1} + 2y_2^{k-1}t = y_1^k + 2y_2^k t \\ z_1^{k-1} + 2z_2^{k-1}t = z_1^k + 2z_2^k t \\ \quad k = 2, 3, \dots \dots, n_s \end{cases} \quad (12)$$

All these constraints are treated as soft (weighted) constraints. The bundle adjustment solution determines the polynomial coefficients instead of the exterior orientation parameters themselves.

The overall estimation model results in:

$$\begin{cases} v_c = Ax_{dis} + B_s x_s + B_d x_d + Cx_g - l_c; & P_c \\ v_1 = A_1 x_{dis} & -l_1; & P_1 \\ v_2 = A_2 x_{dis} & -l_2; & P_2 \\ v_s = \quad x_s & -l_s; & P_s \\ v_d = \quad x_d & -l_d; & P_d \\ v_g = \quad x_g - l_g; & P_g \end{cases} \quad (13)$$

The first equation of this system is the linearized observation equation of (7) and the following two equations are derived from the two kind of constraints; x_{dis} contains the unknown translational displacement correction terms (ΔX, ΔY, ΔZ) for all spline sections; x_s and x_d are the unknown INS shift and drift terms respectively; x_g is the ground coordinate vector; A, A_1, A_2, B_s, B_d and C are the corresponding design matrices; v, l and P are the respective residual and discrepancy vectors and weight matrices. Through this consequent weighting scheme much flexibility is obtained with respect to the modeling of different trajectory conditions.

4.3 *Lagrange Interpolation Model (LIM)*

EBNER et al. 1992 developed the principle of orientation images or orientation fixes for the geometric in-flight calibration of MOMS imagery. This method is based on collinearity equations and the exterior orientation parameters are determined in the so-called orientation fixes, which are introduced at certain time intervals. Between the orientation fixes, the exterior orientation parameters of an arbitrary scan line are interpolated using Lagrange polynomials. All unknown orientation parameters for these orientation fixes are estimated in a least squares adjustment procedure, and the parameters for each individual scan line are interpolated with its neighboring orientation fixes. The general form of the n-th order Lagrange polynomial is given as

$$P_n(t) = \sum_{i=0}^{n} P(t_i) \prod_{j=0; j \neq i}^{n} \frac{t - t_j}{t_i - t_j} \quad (14)$$

Where $P_n(t)$ at time t is interpolated from the values $P(t_i)$ at the $n + 1$ neighboring orientation fixes with time t_i; $P_n(t)$ is any of the six exterior orientation parameters for a scan line at time t.

The interpolation function of order three has attracted most attention (EBNER et al. 1992, FRASER & SHAO 1996). In our experiments, we modified and adopted this method according to our sensor model with the provision of auxiliary position/attitude data generated by the GPS/INS system. In our case third-order Lagrange polynomials are used to model the aircraft attitude values (Ω, Φ, K) instead of the translational displacement correction terms (ΔX, ΔY, ΔZ) because the former are observations from the system and are related to the translational terms by equations (5). Linear Lagrange polynomials are used to model the INS errors ($\Delta\omega$, $\Delta\varphi$, $\Delta\kappa$) because of their locally linear systematic pattern (FRASER & SHAO 1996).

After combining equations (7) and (14), the following observation equations for the combined triangulation procedure can be formed:

$$\begin{cases} v_c = Ax_a + Bx_{INS} & + Cx_g - l_c; & P_c \\ v_t = \quad x_{INS} + B_s x_s + B_d x_d & -l_t; & P_t \\ v_s = \quad x_s & -l_s; & P_s \\ v_d = \quad x_d & -l_d; & P_d \\ v_g = \quad x_g - l_g; & P_g \end{cases} \quad (15)$$

The first equation of this system is the linearized observation equation of (7) and the se-

cond is a constraint which models the INS error terms in the whole trajectory as shift and drift terms. P_t controls the weight of this constraint. x_a is the unknown attitude parameter vector (Ω, Φ, K) of the aircraft for the orientation fixes; x_{INS} is the unknown INS error $(\Delta\omega, \Delta\varphi, \Delta\kappa)$ vector for the orientation fixes; x_s and x_d are the unknown INS shift and drift terms respectively; x_g is the ground coordinates vector; A, B, B_s, B_d and C are the corresponding design matrices; v, l and P are the respective residual and discrepancy vectors and weight matrices.

If we have f orientation fixes and p tie/control points, there are $6 \times f + 3 \times p + 6$ unknowns to be estimated in bundle adjustment. The selection of the number of orientation fixes depends on many factors. The software package ORIMA of LH Systems for their three-line scanner ADS40 triangulation procedure argues that the interval between two neighboring orientation fixes must be shorter than the ground distance corresponding to the „short base" (the distance between the nadir and backward image lines) of the ADS40. For the TLS system, this corresponds to 3000–3600 scan lines. From our experiences, the orientation fixes interval of 2000 scan-lines (4 seconds flight time) is appropriate to model the TLS trajectory. The accuracy does not improve anymore by using a smaller interval below 1500 scan lines.

5   Tie Point Extraction

The DGR method, because of its low number of unknown orientation parameters (9), can work with only few tie and control points. If there are enough control points one could even do without extra tie points altogether. However, the triangulation procedures with the LIM and PPM trajectory models need a large number of tie points. A software package has been developed for tie point extraction from TLS imagery. Tie points can thus be extracted semi-automatically or fully automatically. Problems with fully automatic extraction might occur in low image contrast areas and forest areas. Also, the blunders need to be detected and

deleted. The image matching process is done in image space and exploits all three, i.e. forward, nadir and backward TLS images. In order to achieve sub-pixel accuracy the Least Squares Matching is used. The procedure runs as follows:

● The Foerstner interest operator is used to select well defined feature points that are suitable for image matching. When working in the semi-automatic mode, the user can select the match points in the nadir image. If the software works in fully automatic mode, the nadir-view image will be divided into small image windows (21×21 pixels) and then only one feature point will be extracted in each image window. In our implementation, the threshold for the Foerstner parameter roundness has been set to 0.85, the gray value variance of the image window is not allowed to drop below 20.

● Pixel accuracy level conjugate points are generated using the maximum of the normalized correlation coefficient. The positioning of the search areas is determined by using the already known tie/control points in the neighborhood. Image pyramids and a matching strategy based on region growing, which takes the already manually measured control points as seed points are used to get these approximate points. The threshold of the normalized correlation coefficient is 0.85.

● Least squares matching is finally used to refine the image coordinates of the tie points in order to achieve sub-pixel accuracy.

In our first test the semi-automatic tie point extraction strategy was used. Several hundreds of tie points are thus extracted in an interactive way. These tie points are introduced into the combined aerial triangulation procedure. In addition, the results of fully automatic tie point extraction are also reported.

6   Experimental Results

6.1 *Image Data*

In our experiments, TLS images in forward, nadir and backward views of Japan's GSI test area together with the position and attitude data of the sensor were used to eva-

luate the geometric accuracy of the TLS imagery and our triangulation approaches. The GSI test area is covered by a strip of 650 m × 2500 m. The footprint is about 5.6 cm. There are two versions of the trajectory data for the GSI area. One is the data that includes the GPS-camera displacement corrections and the other does not. The test area is relatively flat. All the 48 control points are signalized marks on the ground or on the top of buildings. The control points were measured using GPS and conventional total stations. The obtained accuracy was reported as 2 cm for the horizontal and 3 cm for the vertical components. The image coordinates of these points were measured manually in the TLS images.

6.2 Results of the DGR Model

The experiment with the DGR trajectory model was designed to test the overall performance of the whole sensor system. In a first step, the offsets between GPS receiver and the perspective center of the TLS camera, the INS shift and drift error terms and the misalignment angles were estimated by using a subset of the control points plus some check points, used as tie points here. Then these parameters were used to calculate the ground coordinates of the remaining checkpoints by equation (7). Tab. 2 gives the RMS values of the discrepancies for the checkpoints for the study area. $\hat{\sigma}_0$ is the estimated standard deviation of unit weight.

Tab. 2: RMS values of checkpoint residuals for triangulation adjustments with the DGR trajectory model.

GPS-Camera Corrections	Control + Check Points	$\hat{\sigma}_0$ (μ)	RMS X (cm)	RMS Y (cm)	RMS Z (cm)
No	4+44	13.7	7.2	8.8	17.2
	6+42	13.7	7.3	8.7	17.1
	8+40	13.8	7.2	8.8	16.6
	12+36	13.8	7.1	8.5	16.5
	18+30	13.8	7.2	8.4	16.3
	24+24	13.9	7.2	8.3	16.2
Yes	4+44	9.1	5.4	6.3	9.4
	6+42	9.1	5.4	6.1	9.1
	8+40	9.2	5.1	5.4	8.7
	12+36	9.2	5.5	6.0	8.6
	18+30	9.2	4.9	5.5	8.7
	24+24	9.3	4.9	5.4	8.8

The triangulation procedure gives better results when the GPS-camera displacement corrections are applied. With different numbers and distributions of control points, 4.9–6.3 cm and 8.6–9.4 cm absolute accuracy in planimetry and height are achieved. Due to the fact that the GPS-camera displacement corrections for each scan line are variable with time (equation (5)), the accuracy is worse with the trajectory data without the displacement corrections. Thus, 7.1–8.8 cm and 16.2–17.2 cm absolute accuracy in planimetry and height is achieved here. These results prove that the attitude data for the aircraft should be recorded and the GPS-camera displacement corrections need to be applied, at least for the DGR model, to achieve a reasonable accuracy.

However, the results are widely independent on the number of control points. For low accuracy applications, the DGR model is a good solution because it can achieve reasonable results with only 4–8 well-distributed control points. Also, the triangulation results with the DGR model can be used to detect and delete large-size blunders in the fully automatic tie point generation procedure.

6.3 Results of the PPM and LIM Models

Similar to the situation with frame-based images, the triangulation accuracy of TLS images with the PPM and LIM trajectory models is affected by the number of control points and their distribution. Also, the number of piecewise sections and orientation fixes will affect the resulting accuracy. Tab. 3 and 4 provide a summary of the accuracies obtained for the study area with the PPM and LIM models respectively. In these results, the tie points were measured semi-automatically. Tab. 5 gives the results with tie points extracted fully automatically.

With different numbers of spline sections or orientation fixes, 2.6–6.0 cm and 4.9–11.7 cm absolute accuracy in planimetry and height is attained using the PPM and LIM models. These results show that a ground point determination of 0.5–1.2 pixel accuracy in planimetry and 0.7–2.1 pixel

Tab. 3: RMS values for triangulation with the PPM trajectory model.

No. of Sections (Lines/Int.)	Control+Check+Tie Points	$\hat{\sigma}_0$ (μ)	RMS X (cm)	RMS Y (cm)	RMS Z (cm)
3 (13610)	6+42+206	9.4	6.0	5.1	11.2
	12+36+206	9.5	5.3	4.8	10.9
	18+30+206	9.5	5.0	4.6	9.6
	24+24+206	9.4	4.9	4.7	9.1
	48+0+206	9.5	4.9	4.4	8.6
5 (8166)	6+42+206	7.8	5.9	5.6	10.7
	12+36+206	7.9	4.7	4.8	8.7
	18+30+206	8.0	4.7	4.8	8.7
	24+24+206	8.0	4.5	4.3	8.5
	48+0+206	8.1	4.0	4.1	8.2
11 (3712)	6+42+206	6.1	6.0	6.0	9.7
	12+36+206	6.3	4.9	4.6	8.7
	18+30+206	6.3	4.5	4.3	8.3
	24+24+206	6.4	4.3	4.1	7.9
	48+0+206	6.5	3.6	3.9	6.8
21 (1944)	6+42+206	4.8	5.3	5.6	8.8
	12+36+206	4.9	5.1	4.9	8.5
	18+30+206	5.0	4.7	4.1	7.9
	24+24+206	5.1	4.0	3.9	6.7
	48+0+206	5.3	3.5	3.1	6.0

accuracy in height are achieved. Given the same number of GCPs, the LIM model returns slightly better results than the PPM model, both in σ_o and in the RMS values for the check points. When evaluating the absolute accuracy level it should be noted that the signalized control points and check

Tab. 4: RMS values for triangulation with the LIM trajectory model.

No. of OFs (Lines/Int.)	Control+Check+Tie Points	$\hat{\sigma}_0$ (μ)	RMS X (cm)	RMS Y (cm)	RMS Z (cm)
10 (4082)	6+42+206	5.8	4.5	4.5	11.7
	12+36+206	5.8	4.8	4.3	10.3
	18+30+206	5.9	4.2	3.9	8.7
	24+24+206	5.9	3.9	3.8	7.3
	48+0+206	6.0	3.7	3.6	6.4
20 (2040)	6+42+206	4.8	4.3	4.4	9.2
	12+36+206	4.9	4.2	4.1	9.7
	18+30+206	5.0	3.9	4.2	7.2
	24+24+206	5.1	3.4	4.1	6.8
	48+0+206	5.2	3.0	3.7	5.8
30 (1361)	6+42+206	4.6	4.0	4.1	8.8
	12+36+206	4.7	3.9	3.8	8.4
	18+30+206	4.8	3.7	4.1	7.1
	24+24+206	4.9	3.3	3.7	6.5
	48+0+206	5.0	2.8	3.0	5.3
40 (1020)	6+42+206	4.4	3.9	4.0	7.6
	12+36+206	4.4	3.7	3.7	7.4
	18+30+206	4.4	3.2	3.5	6.7
	24+24+206	4.6	3.2	3.5	6.4
	48+0+206	4.8	2.7	2.8	4.9

Tab. 5: RMS values for the triangulation with the LIM trajectory model and fully automatically measured tie points (40 orientation fixes).

Control+Check+Tie Points	$\hat{\sigma}_0$ (μ)	RMS X (cm)	RMS Y (cm)	RMS Z (cm)
6+42+3654	4.8	3.1	3.7	8.2
12+36+3654	4.9	2.9	3.6	7.9
18+30+3654	5.0	2.6	3.4	7.9
24+24+3654	5.1	2.2	3.1	7.7

points are very small in the images (about 3–7 pixels diameter) and they were measured manually, which does not give the best possible accuracy. Also, the GPS-determined reference values were said to have already an inaccuracy of 2 cm in planimetry and 3 cm in height, accounting for roughly 50 % of the error budget.

Tab. 5 shows the triangulation results with the LIM model and fully automatically extracted tie points. In this result, the number of orientation fixes was set to be 40. The number of tie points after blunder cleaning is 3654 (in our experiments 5–10 % blunders are detected and deleted). The accuracy in height is slightly worse than the one with the semi-automatical tie point measurement version. This can be expected because there are some small size blunders left here.

In our systems we get high correlations between the estimated orientation parameters. By analysis of the covariance matrix of the estimated parameters, the correlations between the pitch (roll) values and the positional elements in X (Y) direction reach 90%. Therefore TLS image strips with different flight direction and different flying height should be used to de-correlate the estimated orientation elements, especially the estimated exterior orientation elements and interior orientation parameters, if used in a self-calibration procedure. The results of these works will be reported later.

6.4 *Computing times*

Computing times are of only temporary interest because they depend largely on the computer configuration used and on the status of software optimization. In the following we will give some numbers just for the

purpose of giving the reader some ideas about the coarse amount of CPU times needed to perform tie point extraction and triangulation. The number refer to the computer configuration DELL Optiplex GX1P with Pentium II processor at 450 MHz and 256 MB RAM. Also, at its current stage, the software is not fully optimized concerning speed. Improvements both on the software and hardware side will be made as the project progresses.

The automated extraction of 3654 tie points from an image triplet using crosscorrelation takes 37 min. If the results obtained are refined by least squares matching an additional 80 min is added.

For triangulation with three image strips we obtain:

DGR model:
206 tie points: $< 1/10$ sec
PPM model:
206 tie points, 3 segments: 40 sec
206 tie points, 21 segments: 2.5 min
LIM model:
206 tie points, 5 segments: 20 sec in total
206 tie points, 50 segments: 22 sec per iteration (2−3 iterations)
3654 tie points, 50 segments: 9 min per iteration (2−3 iterations)

In tie point extraction the computing times should depend linearly on the number of points extracted and on the method of matching used.

In triangulation we have to deal with more complex relationships. The main effort goes into the solution of the normal equations. Here the size and the sparsity of the normals is critical. The number of operations (and thus the CPU) goes with the nxb^2 law (n = number of unknowns, b = bandwidth). Therefore the number of segments and the number of tiepoints both have a significant influence. Some additional considerations apply if the inverse of the normals is computed for precision studies (this procedure is implemented, but not included in the given numbers).

7 Conclusions

The sensor model of the Three-Line-Scanner (TLS) system, developed by STARLABO Corporation, Tokyo has been described. Triangulation procedures with three different trajectory models have been developed: (a) Direct georeferencing with stochastic exterior orientations (DGR), (b) Piecewise Polynomials with kinematic model up to second order and stochastic zero and first order continuity constraints (PPM) and (c) Lagrange Polynomials with variable orientation fixes (LIM).

With different numbers and distributions of control points and tie points, 4.9−6.3 cm and 8.6−9.4 cm absolute accuracy in planimetry and height is achieved using the DGR model under the condition that the GPS/camera displacement corrections have been applied. Moreover, with different number of spline sections or orientation fixes, 2.6−6.0 cm and 4.9−11.7 cm absolute accuracy in planimetry and height is attained using the PPM and LIM models. These results show that a ground point determination of 0.5−1.2 pixel accuracy in planimetry and 0.7−2.1 pixel accuracy in height has been achieved. However, with the given data the accuracy limit of the system could not be fully explored, because both the image measurements and the accuracy of control and check points did not present the state-of-the-art.

Furthermore, the backward and forward images suffered under significant image blur, caused by lens imperfections.

The orientation parameter determination using the DGR model has the advantage of stability and needs less ground control points, but the obtained accuracy is better with the PPM and LIM models. This however is penalized by the need to have more well-distributed ground control and tie points with these latter models.

The CPU times indicate, while the software is not yet fully optimized in this respect and while they depend strongly on the computer configuration used, that they impose no real problem. The sensor model and the triangulation of relatively large blocks can be handled in reasonable time.

The major time factor relates to the extraction of tie points. Here high precision results are penalized by additional CPU efforts (least squares matching adds about 200 % CPU time to the crosscorrelation results). This must be compared to the times absorbed by manual measurements, and here we are by many factors faster. However, realistically, real-time performance cannot be expected from such a system.

The future experiments will include the triangulation procedure with self-calibration, using TLS multi- and cross-strips imagery, the detection of the small size blunders, the investigation of the effect of undetected small blunders and other issues. The covariance matrix of the estimated parameters is available for extensive theoretical precision studies of the different system configurations.

Currently, the TLS sensor is being replaced by a new camera, called STARIMAGER SI-200, which features a new, improved lens, 14 400 pixels per line and an additional infrared CCD line in the focal plane. Our future tests will include this new imagery as well.

Acknowledgement

References

BOERNER, A., REULKE, R., SCHEELE, M. & TERZIBASCHIAN, TH., 1997: Stereo Processing of Image Data from an Airborne Three-Line CCD Scanner. – The 3rd International Airborne Remote Sensing Conference and Exhibition, 7–10 July, Copenhagen, Denmark.

CANNON, E., 1994: The Use of GPS for GIS Georeferencing: Status and Applications. – IAPRS, Vol. **30**, Part 2: 163–172, Ottawa, Canada.

CHEN, T., SHIBASAKI, R. & MORITA, K., 2001: High Precision Georeference for Airborne Three-Line Scanner (TLS) Imagery. – 3rd International Image Sensing Seminar on New Developments in Digital Photogrammetry, Sept. 24–27, Gifu, Japan, pp. 71–82.

CRAMER, M., 2000: Genauigkeitsuntersuchungen zur GPS/INS-Integration in der Aerophotogrammetrie. – Dissertation, University of Stuttgart, Stuttgart, 120 pages.

EBNER, H., KORNUS, W. & OHLHOF, T., 1992: A Simulation Study on Point Determination for The MOMS-02/D2 Space Project Using an Extended Functional Model. – IAPRS, Vol. **29**, Part B4: 458–464, Washington, D.C.

FRASER, C.S. & SHAO, J., 1996: Exterior Orientation Determination of MOMS-02 Three-Line Imagery: Experiences with the Australian Test Field Data. – IAPRS, Vol. **31**, Part B3: 207–214, Vienna.

HAALA, N., STALLMANN, D. & CRAMER, M., 1998: Calibration of Directly Measured Position and Attitude by Aerotriangulation of Three-Line Airborne Imagery. – IAPRS, Vol. 32, Part 3: 23–30, Budapest.

LEE, C., THEISS, H.J., BETHEL, J.S. & MIKHAIL, E.M., 2000: Rigorous Mathematical Modeling of Airborne Pushbroom Imaging System. – Photogrammetric Engineering & Remote Sensing, Vol. **66**, No. 4, April, pp. 385–392.

LH Systems ADS40 Airborne Digital Sensor – Digital Image Acquisition for Professionals, available on ftp://ftp.gis.leica-geosystem.com/outgoing/docs/ada/ADS 40_Brochure.pdf

MURAI, S., 2001: Development of Helicopterborne Three Line Scanner with High Performance of Stabilizer and IMU. – 3rd International Image Sensing Seminar on New Development in Digital Photogrammetry, Sept. 24–27, Gifu, Japan, pp. 1–3.

MURAI, S. & MATSUMOTO, Y., 2000: The Development of Airborne Three Line Scanner with High Accuracy INS and GPS for Analysing Car Velocity Distribution. – IAPRS, Vol. **33**, Part B2: 416–421, Amsterdam.

REULKE, R., FRANKE, K.-H., FRICKER, P., POMIERSKI, T., SANDAU, R., SCHOENERMARK, M., TORNOW, C. & WIEST, L., 2000: Target Related Multispectral and True Color Optimization of the Color Channels of the LH Systems ADS40. – IAPRS, Vol. **33**, Part B1: 244–250, Amsterdam.

SANDAU, R., BRAUNECKER, B., DRIESCHER, H., ECKARDT, A., HILBERT, S., HUTTON, J., KIRCHHOFER, W., LITHOPOULOS, E., REULKE, R. & WICKI, S., 2000: Design Principle of The LH Systems ADS40 Airborne Digital Sensor. – IAPRS, Vol. **33**, Part B1: 258–265, Amsterdam.

SCHWARZ, K.P. & WEI, M., 1994: Aided Versus Embedded: A Comparison of Two Approaches to GPS/INS Integration. – Proc. IEEE Position

Location and Navigation Symposium, April 11–15, Las Vegas, pp. 314–321.

SKALOUD, J., 1999: Optimizing Georeferencing of Airborne Survey System by INS/DGPS. – Dissertation, Calgary, Alberta, 210 pages.

WEWEL, F., SCHOLTEN, F. & GWINNER, K., 1999: High Resolution Stereo Camera (HRSC) – Multispectral Data Acquisition and Photogrammetric Data Processing. – 4th International Airborne Remote Sensing Conference and Exhibition, Vol. I: 263–272, Ottawa, Canada.

Anschrift der Autoren:

Prof. Dr. ARMIN GRUEN
ZHANG LI, M.SC.
Institute of Geodesy and Photogrammetry
ETH-Hoenggerberg, CH-8093, Zürich
Switzerland,
e-mail: (agruen,zhangl)@geod.baug.ethz.ch